Fault-tolerant efficient control of six-phase induction generators in wind energy conversion systems with series-parallel machine-side converters

I. Gonzalez, M.J. Duran*, H.S. Che†, E. Levi+, J. Aguado**

**University of Málaga, Spain, igp@uma.es, mjduran@uma.es, jaguado@uma.es*
†University of Malaya, Malaysia, cehase@hotmail.com
+ Liverpool John Moores University, UK, E.Levi@ljmu.ac.uk

Keywords: Wind energy systems, multiphase generators, fault tolerance, efficient control.

Abstract

This work discusses the implementation of an efficient fault-tolerant control in a multiphase wind energy conversion system. The conversion system consists of an asymmetrical six-phase induction generator supplied by four voltage source converters (VSCs) in a hybrid series/parallel configuration. Post-fault operation must preserve the current ratings of the system and should also maximize the generated power by means of a proper flux adjustment. Both requirements are achieved in this work using a non-linear optimization analysis and some modifications in the control scheme. Simulation results confirm the optimal and safe performance of the wind energy system under study.

1 Introduction

Wind energy is currently the most developed renewable energy source, with 282,275 MW of worldwide installed power in 2012 satisfying more than 3% of the global electricity demand. Even though offshore wind farms represent a low percentage of the overall wind power, the growth of this kind of wind installations in 2012 exceeded that of onshore farms. China, UK and Denmark are the main promoters of offshore wind farms [1]. Some of the reasons of the growth of the maritime wind energy are the existence of more stable and stronger winds, the availability of land and the lower visual pollution, to name a few. However, the foundation and grid connection of offshore wind farms are complicated and expensive. Furthermore, the particular location of these installations complicates the maintenance tasks. Focusing on the latter disadvantage, it becomes a major need to design wind energy systems with the capability to operate in the event of a fault. This fault tolerance is precisely one of the main advantages of multiphase generators compared to their three-phase counterparts.

Even though multiphase machines have been mainly suggested for electric drives in the last decade [2], their use as generators in wind energy applications has been recently investigated [3-9]. With the advent of tighter grid codes, full-power wind energy systems are becoming more popular and the use of back-to-back converters allows using multiphase generators in different configurations. Furthermore, the design of larger wind turbines (currently up to 10 MW) and the reliability requirements match the features of multiphase machines due to their capability to split power and provide fault tolerance. The most investigated option has been the use of a six-phase generator (either induction [8] or permanent magnet [9]) supplied by two-level voltage source converters (VSCs). The range of topologies includes parallel [9], series [8] and hybrid series/parallel [10] connection of the converters. Previous investigations on multiphase wind energy systems have been focused on the topology analysis and control aspects in pre- and post-fault situations, but the efficiency improvement of such systems has not been addressed yet.

The improvement in the energetic efficiency of wind energy conversion systems can be achieved with an optimal design of the machines [11-13] or with the implementation of an efficient control [14-23]. The latter approach includes several strategies, such as the search control (SC) [15-19] or loss model control (LMC) [20-23]. Regardless of the approach, the method to improve efficiency is typically based on reducing the magnetic flux in the machine at light loads to reduce the losses at the expense of a slower dynamic response. Search control measures online the input power and iteratively changes the degree of magnetization of the machine until the minimal input power is detected. A usual disadvantage of this method is its slow convergence. To improve the convergence, fuzzy logic can be applied to estimate the optimum step size of the input power and magnetic flux [17-19]. This method is not sensitive to the machine parameters. On the other hand, the loss model control calculates offline the optimum flux level from a theoretical model of the system. For the implementation of this method, it is necessary to know the machine parameters, as they are part of the model. The optimal flux can be obtained analytically when the loss model is simple [20], whereas no analytical techniques can be used when the complexity of the model increases [21-23].

Regardless of the control strategy used, most of these works have been performed for three-phase induction machines in motoring mode [14-16], [18-23]. The literature on the efficiency improvement for multiphase machines in normal operation is scarce [15] and it is non-existent in fault-tolerant mode of operation, either in motoring or generating mode.

Since multiphase systems possess additional degrees of freedom and fault-tolerant operation requires additional restrictions, the extension of the analysis performed for three-phase induction machines is far from being trivial. This work performs the efficiency analysis for the specific hybrid topology of [10] in fault-tolerant mode of operation. The optimum flux is obtained from a nonlinear optimization process and the resulting optimal values are included in the control scheme to improve efficiency in steady state retaining a good dynamic performance. Even though main flux saturation influences the optimal flux level evaluation, it is neglected in this work for the sake of simplicity.

The paper is organized as follows: section II examines the topology under study and its fault-tolerant capability; section III describes the nonlinear optimization procedure and provides the optimal flux for different wind conditions; section IV shows simulation results of a case study in steady state and transient conditions and section V summarizes the main conclusions of the work.

2 Post-fault wind power generation

The system under study consists of a six-phase induction machine fed by four three-phase two-level voltage source converters (VSCs) on the generator side (Fig. 1). Each set of three-phase windings (termed $a_1b_1c_1$ and $a_2b_2c_2$) is connected to two three-phase VSCs operating in parallel (collectively termed VSCs1 and VSCs2). The dc-links of the two parallel VSCs (termed V_{dc1} and V_{dc2}) are then cascaded in series to form an elevated dc-link voltage, which allows the generation at medium voltage on the grid-side [10]. This hybrid topology provides some additional fault tolerance compared to the pure series topology of [3].

The fault situation occurs when leg A_1' of VSCs1 is open circuited. Due to the parallel connection of the converters $A_1B_1C_1$ and $A_1'B_1'C_1'$, phase-a_1 is still fed with leg-A_1 of VSCs1, and consequently the current can still flow. However, maximum phase current in phase-a_1 is now just half of the rated phase current (i.e. $I_n/2$) due to the limitation on the VSCs current rating. If the wind torque is below 25% of the generator rated torque, this limit is not achieved and the wind energy system is not affected by the fault. Above this torque limit, currents in the faulted set of three-phase windings need to remain balanced and to be equally limited in order to avoid power oscillations:

$$i_{a1} = 0.5 \cdot I_n \cdot \cos(\omega t) \quad (1)$$

$$i_{b1} = 0.5 \cdot I_n \cdot \cos(\omega t - 120^0)$$

$$i_{c1} = 0.5 \cdot I_n \cdot \cos(\omega t - 240^0)$$

Since VSCs2 are healthy, there is no current limit in the other set of three-phase windings and the phase currents can be generally expressed as:

$$i_{a2} = k \cdot I_n \cdot \cos(\omega \cdot t - 30^0) \quad (2)$$

$$i_{b2} = k \cdot I_n \cdot \cos(\omega \cdot t - 150^0)$$

$$i_{c2} = k \cdot I_n \cdot \cos(\omega \cdot t - 270^0)$$

where k is a parameter ($0.5 < k < 1$), whose value represents the degree of imbalance in the current sharing between VSCs1 and VSCs2. If $k = 0.5$, the solution is trivial and the maximum post-fault torque is limited to 25% of the rated value. Higher values of k imply non-zero x-y (i.e., non-torque related [2]) currents, but also higher output power.

This additional power can be obtained using the modified control scheme of [10], where an additional controller regulates the value of k which in turn injects non-zero x-y currents. Fig. 2 shows the power curves obtained in [10] for different values of k. This increased output power is however obtained at the expense of an imbalance in the dc-link voltages V_{dc1} and V_{dc2} in order to keep equal active power sharing from both sets of three-phase windings. In steady state $I_{dc1} = I_{dc2}$ and consequently the ratio of dc-link voltages is equal to the ratio of the active powers generated in VSCs1 and VSCs2:

$$\frac{V_{dc1}}{V_{dc2}} = \frac{P_1}{P_2} \quad (3)$$

The active power can be expressed in terms of the stator currents using the double dq model approach:

$$P_1 = -V_{dc1} \cdot I_{dc1} = -\left[v_{\alpha 1} \cdot i_{\alpha 1} + v_{\beta 1} \cdot i_{\beta 1}\right] \quad (4)$$

$$P_2 = -V_{dc2} \cdot I_{dc2} = -\left[v_{\alpha 2} \cdot i_{\alpha 2} + v_{\beta 2} \cdot i_{\beta 2}\right]$$

Considering the relationship between the double dq and the vector space decomposition (VSD) model [8],

$$i_{\alpha 1} = \frac{1}{\sqrt{2}} \cdot (i_\alpha + i_x) \qquad i_{\beta 1} = \frac{1}{\sqrt{2}} \cdot (i_\beta - i_y) \quad (5)$$

$$i_{\alpha 2} = \frac{1}{\sqrt{2}} \cdot (i_\alpha - i_x) \qquad i_{\beta 2} = \frac{1}{\sqrt{2}} \cdot (i_\beta + i_y)$$

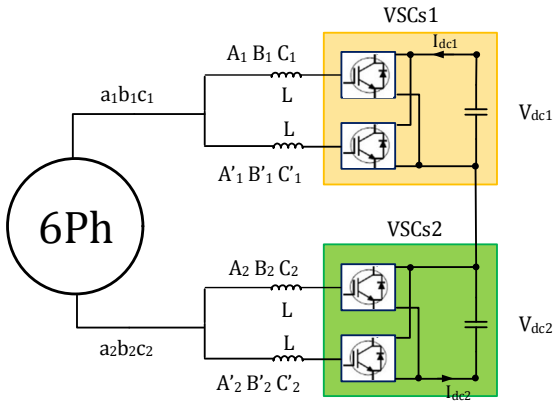

Fig. 1. Six-phase wind generator supplied by a combination of series-parallel converters.

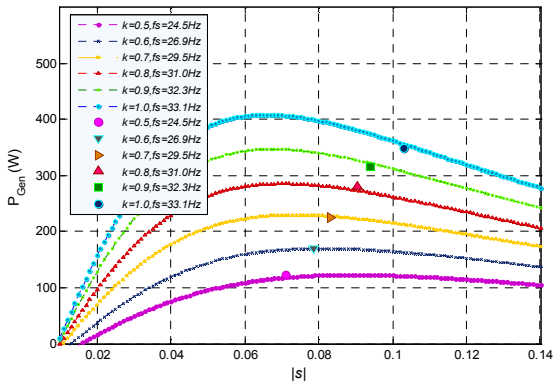

Fig. 2. Wind power generation for increasing values of $\boldsymbol{k}$ in the range $\boldsymbol{k} \in \{\mathbf{0.5-1}\}$.

it is possible to express the active power of (4) in terms of VSD variables. Substituting (5) into (4) and rearranging, the active power can be expressed in terms of common and differential components:

$$P_1 = -\frac{1}{2}[\underbrace{(v_\alpha i_\alpha + v_\beta i_\beta + v_x i_x + v_y i_y)}_{P_{CC}=common\ component} + \underbrace{(v_x i_\alpha + v_\alpha i_x - v_y i_\beta - v_\beta i_y)}_{P_{CD}=differential\ component}] \quad (6)$$

$$P_2 = -\frac{1}{2}[\underbrace{(v_\alpha i_\alpha + v_\beta i_\beta + v_x i_x + v_y i_y)}_{P_{CC}=common\ component} - \underbrace{(v_x i_\alpha + v_\alpha i_x - v_y i_\beta - v_\beta i_y)}_{P_{CD}=differential\ component}]$$

From the VSD steady state equivalent circuit of the induction generator [10], it is possible to express the α-β-x-y voltages in terms of the α-β-x-y currents and impedances:

$$v_\alpha = (Z_\alpha i_\alpha - Z_\beta i_\beta) \qquad v_\beta = (Z_\beta i_\alpha + Z_\alpha i_\beta) \quad (7)$$

$$v_x = (Z_x i_x - Z_y i_y) \qquad v_y = (Z_y i_x + Z_x i_y)$$

$$Z_\alpha = Re(R_s + j \cdot X_{ls} + \frac{1}{\frac{1}{j \cdot X_m} + \frac{1}{\frac{R_r}{s} + j \cdot X_{lr}}})$$

$$Z_\beta = Im(R_s + j \cdot X_{ls} + \frac{1}{\frac{1}{j \cdot X_m} + \frac{1}{\frac{R_r}{s} + j \cdot X_{lr}}})$$

$$Z_x = R_s \qquad Z_y = X_{ls}$$

where R_s and R_r are the stator and rotor resistances, X_{ls} and X_{lr} are the stator and rotor leakage reactances, X_m is the magnetizing reactance and s is the slip. Introducing (7) into (6), the common and differential components of the active power can be expressed as:

$$P_{CC} = -\frac{3}{2} I_n^2 [Z_\alpha (0.25 + 0.5k)^2 + Z_x (0.25 - 0.5k)^2] \quad (8)$$

$$P_{CD} = -\frac{3}{2} I_n^2 (Z_\alpha + Z_x)(0.25^2 - 0.5^2 k^2)$$

Replacing (8) into (6) and (3), the imbalance between the dc-link voltages becomes a function of k and the impedances:

$$\frac{V_{dc1}}{V_{dc2}} = \frac{Z_\alpha (0.25k + 0.125) - Z_x (0.25k - 0.125)}{Z_\alpha (0.5k^2 + 0.25k) + Z_x (0.5k^2 - 0.25)} \quad (9)$$

Fig. 3 shows the dc-link voltages obtained in numerical simulations [10] compared to the analytical voltages calculated from (9) for different values of k, with 600 V dc-link voltage in pre-fault operation. To sum up, it is possible to extract additional power in post-fault situation (Fig. 2) provided that the system ratings allow a certain degree of dc-link voltage imbalance (Fig. 3). However, it should be noted that the above shown results are obtained setting a constant flux reference, which is not an optimal solution. The next section explores how the system can maximize the output power when both the flux and current imbalance are optimally selected for each operating point.

3 Post-fault flux optimization

The control techniques that adapt the degree of magnetization to the machine's torque in order to minimize losses are broadly called techniques for energy efficient control. These techniques have been widely studied for three-phase induction motor drives where flux weakening at light loads in the base speed region is known to improve efficiency at the expense of a slower dynamic response [14-16], [18-23].

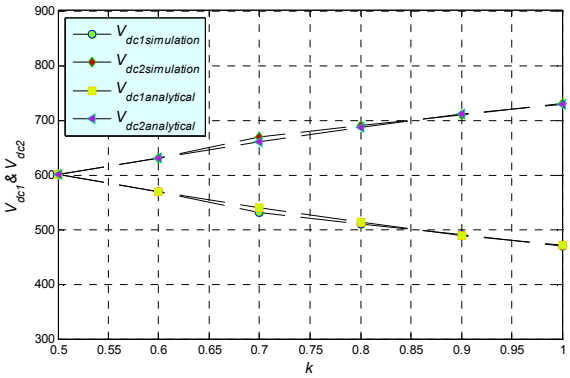

Fig. 3. Analytical and simulated dc-link voltages versus k.

The magnetic flux that provides minimum losses is commonly calculated offline for different loading conditions and these values are then used online for efficient operation. Compared to the standard techniques for three-phase electrical drives, the present study presents some differences:

1) The machine is operated as a generator and consequently the aim of the optimization is not minimizing losses but optimizing the output power.
2) The use of multiphase generators provides additional degrees of freedom to the system complicating the optimization procedure.
3) The fault-tolerant operation includes additional restrictions in order to maintain the systems ratings.

Even though analytical solutions have been obtained in three-phase electrical drives [20], the derivation of an analytical solution for the optimal flux becomes difficult in this case due to the above mentioned features. For this reason the problem is solved using nonlinear optimization techniques. From the optimization point of view, the induction generator model is a nonlinear programming problem [24], as it is defined by nonlinear equations. This kind of problems can be solved with different techniques that are usually included in commercial optimization software. The software used in this work is *GAMS* [25], which allows solving nonlinear problems by defining an objective function, a model of the system and an optimization algorithm (see Fig. 4).

The model implemented in GAMS uses the parameters defined in table I and includes both the equations of the six-phase wind generator and the equations of the indirect field oriented control (IFOC):

$$i_d = \frac{a \cdot \lambda_{rated}}{L_m}$$

$$i_q = (T_e \cdot (L_m + L_{lr}))/(P \cdot L_m \cdot a \cdot \lambda_{rated}) \quad (10)$$

$$|I_{dq}| = \sqrt{(i_d^2 + i_q^2)}$$

$$|I_{dq}| = \sqrt{3} \cdot I_n \cdot (0.5k + 0.25)$$

where parameter a represents the percentage of the rated flux used at each operating point.

The rotation speed of the rotor (ω_r) is defined by the maximum power point tracking (MPPT) algorithm [26], whereas the stator frequency and the slip can be obtained from the IFOC equations:

$$\omega_r = \frac{60}{2 \cdot \pi}\sqrt{-\frac{T_e}{K_{OPT}}} \qquad \omega_{sl} = \frac{L_m \cdot R_r \cdot I_q}{(L_m + L_{lr}) \cdot a \cdot \lambda_{rated}}$$

$$\omega_s = \omega_r \cdot \frac{2 \cdot P \cdot \pi}{60} + \omega_{sl} \qquad |s| = |\omega_{sl}/\omega_s| \qquad (11)$$

$$X_m = \omega_s \cdot L_m; \quad X_{ls} = \omega_s \cdot L_{ls}; \quad X_{lr} = \omega_s \cdot L_{lr}$$

Finally, the VSD equivalent circuits of the multiphase generator are used to calculate the generated power and the losses for every operating point:

$$P_{wt} = 3 \cdot I_n^2 \cdot \frac{R_r}{s} \cdot X_m^2 \cdot \frac{(0.5k + 0.25)^2}{\left(\frac{R_r}{s}\right)^2 + (X_m + X_{lr})^2}$$

$$P_{loss} = 3 \cdot I_n^2 \cdot R_s \cdot ((0.5k + 0.25)^2 + (0.5k - 0.25)^2) \qquad (12)$$

$$P_{Gen} = P_{wt} - P_{loss}$$

where P_{wt} is the input power provided by the wind turbine (neglecting mechanical losses), P_{loss} are the copper losses associated to the different currents flowing in the generator and P_{Gen} is the output power generated by the system. The objective function is to maximize the wind power P_{Gen} generated by the system, by using a magnetic flux appropriate for each operating point. The optimization method *CONOPT* [25] included in GAMS is used in this work because it is suitable for nonlinear problems with few degrees of freedom and a low number of variables.

The model of (10)-(12) is solved in the optimization problem (Fig. 4) for increasing values of T_{wind}, within the range $-5.82\ \text{Nm} < T_{wind} < -2.85\ \text{Nm}$. These values match a range from $I_n/2$ to I_n of $i_{a2}i_{b2}i_{c2}$ in post-fault situation. The optimization procedure performed with GAMS provides the optimal percentage of magnetic flux (a) for different input torque values (see Fig. 5). The optimal magnetic flux for different operating points can be approximated using a linear regression that provides the reference magnetic flux in post-fault situation as:

$$a^* = 0.0819 \cdot |T_{wind}| + 0.3461 \qquad (13)$$

In order to avoid undesirable oscillations of the reference flux in transient states, the control uses a low-pas filter with a cut-off frequency of 10 rad/s for the input torque of (13). It must be emphasised that the nonlinear optimization simultaneously considers that both the flux (a) and the current imbalance (k) can vary to achieve maximum output power. At the same time, current constrains for each phase are included as restrictions of the nonlinear programming problem.

4 Simulation results

This section analyses the outcomes obtained from the simulation of the multiphase wind energy conversion system both in steady state and transient conditions. Steady-state operation is considered first, in the forthcoming sub-section.

Machine parameters			
R_s = 10 Ω	R_r = 6.3 Ω	J = 0.04 kg·m²	P = 2
L_{ls_dq} = 0.04 H	L_{lr} = 0.04 H	L_m = 0.42 H	L_{ls_xy} = 0.04 H
$I_n = 3\ A$	$K_{OPT} = 0.000372$		

Table 1. Wind generator parameters.

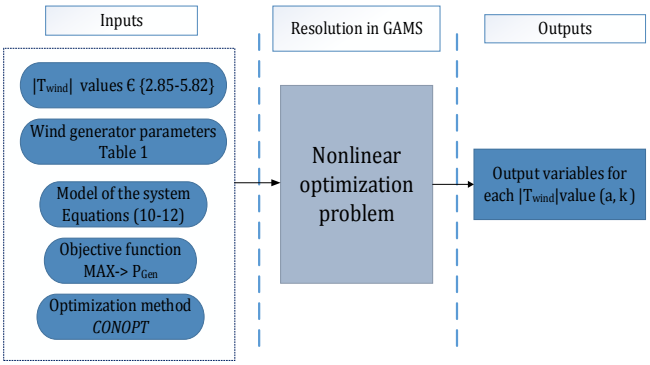

Fig. 4. Schematic of the nonlinear optimization problem.

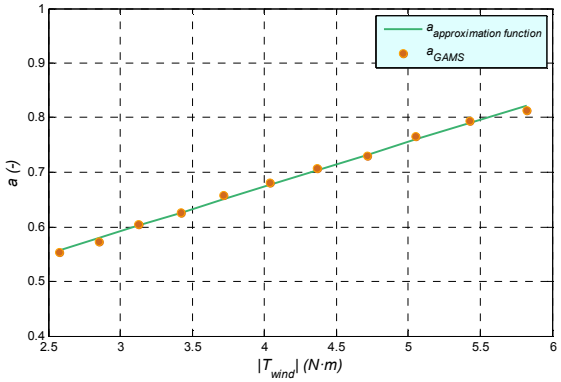

Fig. 5. Optimal percentage of magnetic flux versus the input torque (T_{wind}).

4.1 Steady-state performance

The simulations use the generator parameters defined in table I. The converters are assumed to be ideal and operate at 2 kHz, while the dc-link voltages ($V_{dc1}$and V_{dc2}) are set to 600 V in pre-fault situation. The first test considers steady-state operating points for increasing wind torque values that make parameter k vary from 0.5 to 1. Fig. 6 shows the active power given by the simulations compared to the theoretical power curve for the same operating conditions. It can be noted that the use of the variable flux obtained from the optimization and defined by (13) causes the generator to operate with the slip of the maximum power point, this being in contrast with the limitation given by the use of a constant degree of magnetization [10] (see Fig. 2).

The benefit acquired with the introduction of the efficient control can be further highlighted by representing the power obtained with invariant magnetic flux (59% of the rated value, as in [10]) and variable magnetic flux of (13) versus the modulus of the i_{b2} current, Fig. 7. The range of values represented for i_{b2} (from 1.5 to 3 A) matches a range from 0.5 to 1 for k. As it can be observed in Fig. 7, the generated power for the same rms stator currents is higher when flux is optimized, with a gain in power close to 50% for $k = 1$. Consequently, the efficient control allows a significant increase in the post-fault output power for the same current rating of the system.

To complete the steady state analysis, the dc-link voltage V_{dc2} is represented versus the generated power (P_{Gen}) considering constant flux (59% of the rated value) and variable (optimized) flux. Fig. 8 shows that, for the same imbalance of the dc-link voltages, the variable flux of (13) provides higher

generated power. This implies that optimal flux regulation allows generating the same output power in post fault-situation with a decrease in the oversizing of the converters.

4.2 Transient performance

The next test verifies the dynamic response of the system when sudden changes in the input wind torque appear due to wind gusts (Fig. 9a). Since the MPPT algorithm is activated, the speed reference is also adapted to the wind torque variations (Fig. 9b) in order to ensure maximum power extraction. The system is simulated to be healthy until the fault in leg-A1' of VSCs1 occurs a t = 1 s. Fig. 9c shows the changes in the magnetic flux reference obtained from (13) when the input wind torque varies. This variation of the flux reference also affects the value of the d-current (Fig. 9d) and minimizes the stator currents (Fig. 9e) for the given generated power. Fig. 9 shows an overall good current and speed tracking, indicating a satisfactory dynamic response.

5 Conclusion

The application of an efficient control to a multiphase energy conversion system with a hybrid series-parallel topology reduces the required post-fault derating of the system. The variation of the magnetic flux with the input torque improves the achievable generated power up to 50%. This gain in generated power after a fault can have a relevant advantageous economic impact in offshore wind energy systems, where maintenance cannot be performed instantaneously.

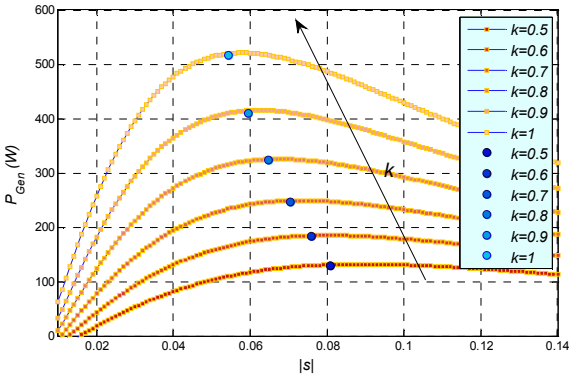

Fig. 6. Wind power generation for increasing values of $\boldsymbol{k}$ in the range $\boldsymbol{k} \in \{\mathbf{0.5-1}\}$ and the magnetic flux is variable.

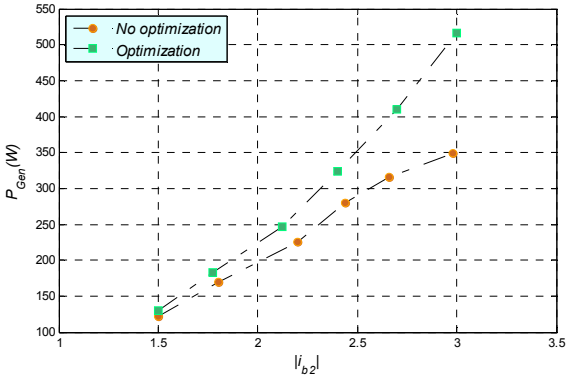

Fig. 7. Power generated versus $\boldsymbol{i_{b2}}$ in post-fault situation.

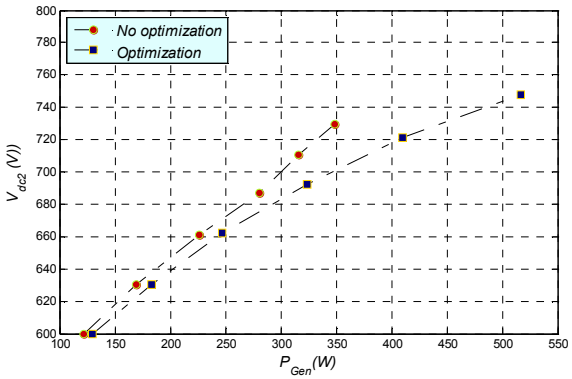

Fig. 8. $\boldsymbol{V_{dc2}}$ voltage versus generated power.

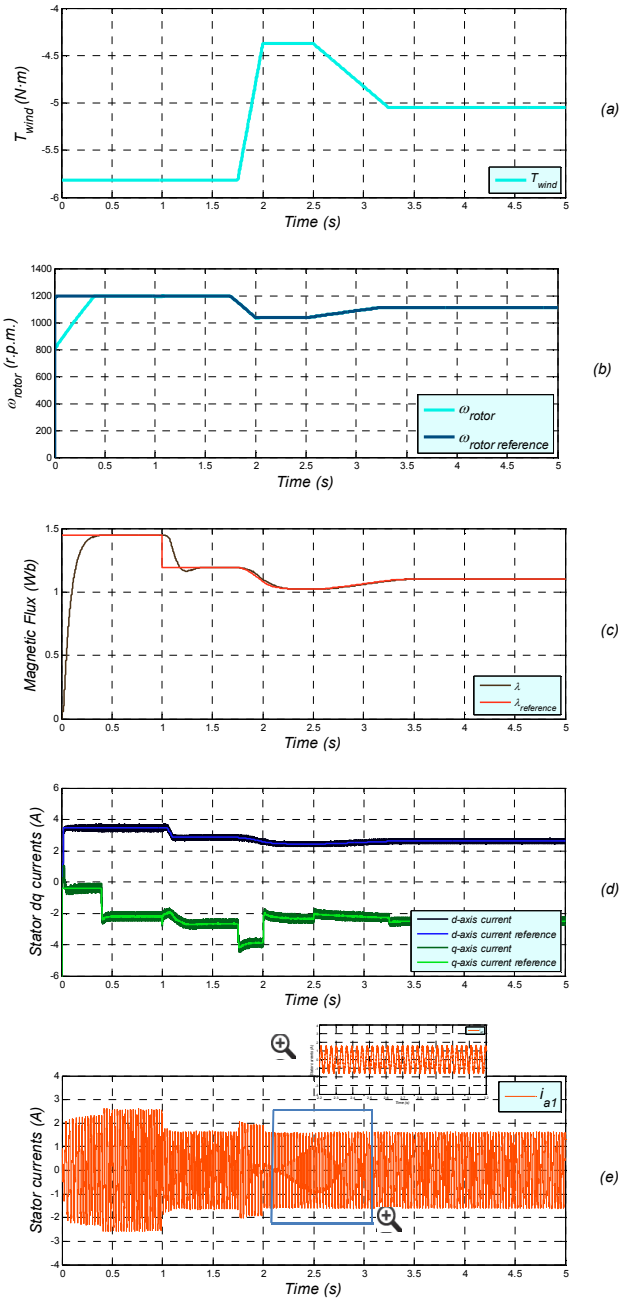

Fig. 9. Input torque (T_{wind}), rotor speed (ω_{rotor}) magnetic flux (λ), d-q currents and phase current $\boldsymbol{i_{a1}}$ in the event of a wind gust and VSC1 fault at t = 1s.

References

[1] World wind energy association, "Annual report 2012". Available: http://wwindea.org.

[2] E. Levi, R. Bojoi, F. Profumo, H. A. Toliyat, and S. Williamson, "Multiphase induction motor drives - a technology status review," *IET Electric Power Applications*, vol. 1, no. 4, pp. 489-516, 2007.

[3] M. J. Duran, S. Kouro, B. Wu, E. Levi, F. Barrero, and S. Alepuz, "Six-phase PMSG wind energy conversion system based on medium-voltage multilevel converter," in *Proc. Eur. Conf. on Power Electronic and Applications EPE*, CD-ROM, 2011.

[4] G. K. Singh, A. Senthil Kumar, and R. P. Saini, "Selection of capacitance for self-excited six-phase induction generator for stand-alone renewable energy generation," *Energy*, vol. 35, no. 8, pp. 3273-3283, 2010.

[5] S. Brisset, D. Vizireanu, and P. Brochet, "Design and optimization of a nine-phase axial-flux PM synchronous generator with concentrated winding for direct-drive wind turbine," *IEEE Trans. on Industry Applications.*, vol. 44, no. 3, pp. 707-715, 2008.

[6] A. Di Gerlando, G. Foglia, M. F. Iacchetti, and R. Perini, "Analysis and test of diode rectifier solutions in grid-connected wind energy conversion systems employing modular permanent-magnet synchronous generators," *IEEE Trans. on Industrial Electronics*, vol. 59, no. 5, pp. 2135-2146, 2012.

[7] Z. Zhang, Y. Yan, S. Yang, and Z. Bo, "Development of a new permanent-magnet BLDC generator using 12-phase half-wave rectifier," *IEEE Trans. on Industrial Electronics*, vol. 56, no. 6, pp. 2023-2029, 2009.

[8] H.S. Che, W.P. Hew, N.A. Rahim, E. Levi, M. Jones, and M.J. Duran, "A six-phase wind energy induction generator system with series-connected DC-links," in *Proc. IEEE Power Electr. for Distributed Generation Systems PEDG*, pp. 26-33, 2012.

[9] Z. Xiang-Jun, Y. Yongbing, Z. Hongtao, L. Ying, F. Luguang, and Y. Xu, "Modelling and control of a multi-phase permanent magnet synchronous generator and efficient hybrid 3L-converters for large direct-drive wind turbines," *IET Electric Power Applications*, vol. 6, no. 6, pp. 322-331, 2012.

[10] I. Gonzalez, M.J. Duran, H.S. Che, E. Levi, and F. Barrero, "Fault-tolerant Control of Six-phase Induction Generators in Wind Energy Conversion Systems with Series-Parallel Machine-side Converters," *39th Annual Conference of the IEEE IES IECON2013*, Vienna (Austria), pp. 5274-5279, 2013.

[11] W. Wei, M. Kiani, and B. Fahimi, "Optimal design of doubly fed induction generators using field reconstruction method," *IEEE Trans. on Magnetics*, vol. 46, no. 8, pp. 3453-3456, 2012.

[12] J.P. Wieczorek, O. Gol, and Z. Michalewicz, "An evolutionary algorithm for the optimal design of induction motors," *IEEE Trans. on Magnetics*, vol. 34, no. 8, pp. 3882-3887, 2002.

[13] K. Min-Kyu, L. Cheol-Gyu, and J. Hyun-Kyo, "Multiobjective optimal design of three-phase induction motor using improved evolution strategy," *IEEE Trans. on Magnetics*, vol. 34, no. 5, pp. 2980-2983, 2002.

[14] C. Thanga Raj, S. P. Srivastava, and P. Agarwal, "Energy efficient control of three-phase induction motor - a review," *International Journal of Computer and Electrical Engineering*, vol. 1, pp. 61-71, 2009.

[15] A. Taheri, A. Rahmati, and S. Kaboli, "Efficiency improvement in DTC of six-phase induction machine by adaptive gradient descent of flux," *IEEE Trans. on Power Electronics*, vol. 27, pp. 1552-1562, 2012.

[16] D. S. Kirschen, D. W. Novotny, and T. A. Lipo, "Optimal efficiency control of an induction motor drive," *IEEE Trans. on Energy Conversion,* vol. 2, no. 1, pp. 70-76, 1987.

[17] A. Mesemanolis, C. Mademlis, and I. Kioskeridis, **"**High efficiency control for a wind energy conversion system with induction generator," *IEEE Trans. on Energy Conversion*, vol. 27, no. 4, pp. 958-967, 2012.

[18] M.G. Simoes, B.K. Bose, and J. Spiegel, "Fuzzy logic based intelligent control of a variable speed cage machine wind generation system,**"** *IEEE Trans. on Power Electronics*, vol. 12, no. 1, pp. 87–95, 1997.

[19] B. K. Bose, N. R. Patel, and K. Rajashekara, "A neuro-fuzzy-based on-line efficiency optimization control of a stator flux-oriented direct vector-controlled induction motor drive," *IEEE Trans. on Industrial Electronics,* vol. 44, no. 270-273, 1997.

[20] I. Takahashi, and T. Noguchi, "A new quick-response and high efficiency control strategy of an induction motor," *IEEE Trans. on Industry Applications*, vol. 22, pp. 820-827, 2006.

[21] R.D Lorenz, and S.-M Yang, **"**Efficiency-optimized flux trajectories for closed-cycle operation of field-orientation induction machine drives," *IEEE Tran.s on Industry Applications*, vol. 28, no. 3, pp. 574-580, 1992.

[22] S.K. Sul, and M.H. Park, "A novel technique for optimal efficiency control of a current-source inverter-fed induction motor," *IEEE Trans. on Power Electronics*, vol. 3, no. 2, pp. 192-199, 1988.

[23] Q. Zengcai, M. Ranta, M. Hinkkanen, and J. Luomi, "Loss-minimizing flux level control of induction motor drives," *IEEE Trans. on Industry Applications*, vol., 48, pp., 952-961, 2012.

[24] E. Castillo, A. Conejo, P. Pedregal, R. Garcia, and N. Alguacil, "Building and Solving Mathematical Programming Models in Engineering and Science," *Editorial Hardcover*, 2002.

[25] GAMS web, "A User's Guide", Available: http://gams.com/docs/

[26] B. Wu, Y. Lang, N. Zargari, and S. Kouro, "*Power conversion and control of wind energy systems*," IEEE Press - John Wiley and Sons, Hoboken, NJ, 2011.